

# Blind Deconvolution in Dynamic Contrast-Enhanced MRI and Ultrasound\*

Radovan Jiřík<sup>1</sup>, Karel Souček<sup>2,3</sup>, Martin Mézl<sup>4,5</sup>, Michal Bartoš<sup>4,6</sup>, Eva Dražanová<sup>1</sup>, František Dráfi<sup>9</sup>,  
Lucie Grossová<sup>1,4</sup>, Jiří Kratochvíla<sup>4</sup>, Ondřej Macíček<sup>4</sup>, Kim Nylund<sup>7</sup>, Aleš Hampl<sup>3,9</sup>,  
Odd Helge Gilja<sup>7,10</sup>, Torfinn Taxt<sup>8</sup>, Zenon Starčuk, jr.<sup>1</sup>

**Abstract**—This paper is focused on quantitative perfusion analysis using MRI and ultrasound. In both MRI and ultrasound, most approaches allow estimation of rate constants (Ktrans, kep for MRI) and indices (AUC, TTP) that are only related to the physiological perfusion parameters of a tissue (e.g. blood flow, vessel permeability) but do not allow their absolute quantification. Recent methods for quantification of these physiological perfusion parameters are shortly reviewed. The main problem of these methods is estimation of the arterial input function (AIF). This paper summarizes and extends the current blind-deconvolution approaches to AIF estimation. The feasibility of these methods is shown on a small preclinical study using both MRI and ultrasound.

## I. INTRODUCTION

Perfusion imaging is an important diagnostic tool used mostly in oncology, neurology and cardiology, to assess the perfusion status of the tissue on a capillary level, e.g. assessment of angiogenesis, ischemic regions and inflammation. This work is focused on clinical and preclinical dynamic contrast-enhanced magnetic resonance and ultrasound imaging (DCE-MRI and DCE-US). In these methods, contrast-agent concentration time curves are derived from the acquired image sequences for each tissue region of interest (ROI, e.g. the whole tumor or each pixel/voxel). In quantitative DCE-MRI, these tissue curves are approximated by a pharmacokinetic model. The ultimate goal is to estimate the physiological perfusion parameters, such as blood flow,

$F_b$ , blood volume,  $v_b$ , vessel permeability-surface product,  $PS$ , and extravascular-extracellular space volume,  $v_e$ .

In DCE-MRI, the usual pharmacokinetic models are the Tofts and extended Tofts models [1]. The estimated perfusion parameters included in these models are the forward transfer constant between blood plasma and the extravascular extracellular (interstitial) space,  $K^{trans}$ , the efflux rate constant from the extravascular extracellular space to blood,  $k_{ep}$  and  $v_e$  (and also  $v_b$  for extended Tofts model). To estimate the complete perfusion-parameter set, including  $F_b$  and  $PS$ , advanced pharmacokinetic models [1] need to be applied, such as the adiabatic approximation to the tissue homogeneity model (ATH), the distributed-capillary adiabatic tissue homogeneity model (DCATH) or the two-compartment exchange model (2CXM). However, the parameter estimation of these advanced pharmacokinetic models requires a high signal-to-noise ratio (SNR) in order not to be ill-conditioned. Furthermore, application of these models assumes a high temporal resolution of the acquisition to capture the vascular-distribution phase of the bolus. These are the main reasons why most quantitative DCE-MRI studies are based on the Tofts or extended Tofts models. This is especially the case for preclinical DCE-MRI, where, to our knowledge, the only use of such models have been [2], [3].

The pharmacokinetic models of quantitative DCE-MRI include the arterial input function (AIF). It is the contrast-agent concentration curve in the arterial input of the tissue ROI. It is one of the major factors causing poor reproducibility of DCE-MRI. There are several approaches to determination of the AIF. The first approach is to derive it from the acquired image sequence as the contrast-agent concentration curve in a large artery [4]. However, such measurement is distorted by flow artifacts, partial volume effect, saturation and T2\* effect. The second approach is to use a population-based AIF [5]. This ignores the differences in the vascular tree between different subjects and depends on the AIF acquisition methods used for creation of these population-based "standards". The third (preclinical) approach is based on analysis of arterial blood samples taken during the bolus application [6] which is a fairly invasive method and suffers from the AIF-shape dispersion (blood samples are taken far from the arterial input of the tissue ROI). The fourth approach is based on a reference tissue (e.g. muscle) [7]. The AIF is estimated from the tissue curve in this reference tissue and the presumably known perfusion parameters. This

\*This study was supported by grants GA102/12/2380, 102/12/1104 of the Czech Science Foundation, by the projects FNUSA-ICRC (CZ.1.05/1.1.00/02.0123) and HistoPARK (CZ.1.07/2.3.00/20.0185) from the European Regional Development Fund and MEYS CR (LO1212), its infrastructure by MEYS CR and EC (CZ.1.05/2.1.00/01.0017) and by ASCR (RVO:68081731)

<sup>1</sup>Institute of Scientific Instruments, AS CR, Brno, Czech Rep. jirik at isibrno.cz

<sup>2</sup>Dept. of Cytokinetics, Institute of Biophysics, AS CR, Brno, Czech Rep.

<sup>3</sup>Center of Biomolecular and Cellular Engineering, International Clinical Research Center, Brno, St. Anne's Univ. Hospital Brno, Czech Rep.

<sup>4</sup>Dept. of Biomedical Engineering, Brno Univ. of Technology, Brno, Czech Rep.

<sup>5</sup>Center of Biomedical Engineering, International Clinical Research Center, St. Anne's Univ. Hospital Brno, Brno, Czech Rep.

<sup>6</sup>Institute of Information Theory and Automation of the ASCR, Praha, Czech Rep.

<sup>7</sup>National Centre for Ultrasound in Gastroenterology, Haukeland University Hospital, Bergen, Norway

<sup>8</sup>Dept. of Biomedicine, University of Bergen, Norway

<sup>9</sup>Dept. of Histology and Embryology, Faculty of Medicine, Masaryk Univ., Brno, Czech Rep.

<sup>10</sup>Dept. of Clinical Medicine, University of Bergen, Bergen, Norway

approach has been shown for the Tofts model. For the advanced pharmacokinetic model, the complete set of perfusion parameters would have to be known which is not very realistic. Another approach to estimation of the AIF is based on blind deconvolution. Imposing prior knowledge (e.g. the pharmacokinetic model, positivity of the contrast-agent concentration curves, model of the AIF) and a suitable initial estimation scheme, it is possible to estimate simultaneously the perfusion parameters and the AIF from the measured tissue ROI contrast-agent concentration curves. This allows estimation a unique AIF for each DCE-MRI acquisition. This approach has been introduced in clinical DCE-MRI as multi-channel deconvolution (multiple tissue ROI signals processed simultaneously) in [8], [9] for the Tofts model and extended to an advanced pharmacokinetic model (ATH) and to the preclinical application group [2], [3].

In DCE-US, quantitative perfusion analysis using a similar concept of pharmacokinetic modeling including the AIF has been introduced recently in [10], [11]. The AIF is measured in a big artery feeding the analyzed tissue. The pharmacokinetic model is simplified by the intravascular character of ultrasound contrast agents. It allows estimation of  $v_b$  and  $F_b$ . However, measurement of the AIF in a blood pool is difficult due to contrast-agent-related attenuation, blood-velocity dependence of the backscattered signal and low spatial resolution of ultrasound images. To avoid this, we have recently proposed a blind-deconvolution approach called bolus & burst [12], [13]. It is based on the following acquisition protocol. Following a contrast-agent bolus application, low-energy imaging pulses are used to record the "bolus-phase" sequence. In the later wash-out phase of the bolus, when the tracer concentration decays rather slowly, a burst pulse sequence is applied to destroy the contrast agent in the imaging plane. The following "replenishment phase" is recorded using low-energy imaging pulses. The assumption of slow decay of the AIF and of zero initial contrast-agent concentration in this replenishment phase are important prior information for blind deconvolution.

This paper presents new extensions to the blind-deconvolution methods of AIF estimation and shows their feasibility on a small preclinical study (group of 4 mice, subcutaneous tumor) for both DCE-MRI and DCE-US. In the DCE-MRI part, our previous blind-deconvolution AIF estimation method [2], [3], based on the ATH pharmacokinetic model and a nonparametric AIF, is extended to a model-based AIF. A new AIF model for preclinical DCE-MRI is introduced. In the DCE-US part, our blind-deconvolution AIF estimation method bolus & burst [12], [13] is extended from clinical to preclinical application by using the same new AIF model as in the MRI part. Another extension of the DCE-US algorithm is generation of perfusion-parameter maps instead of estimation of perfusion-parameters for single large ROIs.

## II. BLIND DECONVOLUTION IN DCE-MRI

The tissue contrast-agent concentration time curve is modeled using a pharmacokinetic model as a convolution of the

AIF and the tissue residue function (TRF), multiplied by blood flow. The TRF is modeled using the ATH model [1]. For AIF, the standard model is a bi-exponential function [14]. While it is probably sufficient for the Tofts and extended Tofts pharmacokinetic models, it is not suitable for advanced pharmacokinetic models, such as the ATH. The need for finer time-domain sampling and more perfusion parameters included in these advanced models require a more flexible AIF model. The new AIF model is a sum of three gamma variate functions:

$$AIF(t) = t^\beta \sum_{n=1}^3 \alpha_n e^{-\tau_n t}, \quad (1)$$

where  $t$  is time,  $\beta$ ,  $\alpha_n$  and  $\tau_n$  are model parameters. Approximation of the contrast-agent concentration time curves by the pharmacokinetic model is formulated as a minimization problem. The criterion function is a sum of the least-squares differences between the contrast-agent concentration time curve and its convolutional model for all channels. The channels represent the tissue regions from which the contrast-agent concentration time curves are extracted (10 channels are used here). Hence, the blind-deconvolution algorithm results in estimates of the TRF parameters (perfusion parameters) of each channel and of the AIF parameters (common for all channels). An alternating optimization scheme is applied where each iteration (10 iterations are used here) consists of two steps: 1. update of the TRF while the AIF is fixed to the actual estimate, 2. update of the AIF while the TRF is fixed to the actual estimate. The substeps are realized using the Active-Set optimization algorithm as implemented in the Matlab<sup>TM</sup> Optimization toolbox (MathWorks, USA), function `fmincon`.

The resulting AIF estimate is scaled so that perfusion analysis of the contrast-agent concentration curve of a reference tissue (here spinal muscle) results in a known literature-based value of  $v_e + v_p$  (here 0.13 ml/g tissue). The sum  $v_e + v_p$  corresponds to the area under the curve of the TRF [2]. The estimated AIF is then subsequently used in the pixel-by-pixel non-blind deconvolution of the whole image sequence to calculate the perfusion-parameter maps.

## III. BLIND DECONVOLUTION IN DCE-US

The pharmacokinetic model used in DCE-US is the same as for DCE-MRI, except for the TRF, which is an exponential function with the time constant being  $F_b/v_b$  [12]. The blind deconvolution algorithm is formulated as minimization of the least-mean-square difference between the measured and modeled signals. One channel (i.e. signal from one ROI) is used. The criterion function is a sum of the bolus and replenishment terms. In the replenishment part, the application of burst is modeled as zero initial condition at the time instant of the replenishment-phase start. Scaling of the AIF estimate is done with respect to a region of the highest area under the curve. The AIF is scaled so that  $v_b$  of this region is 1 ml/g, assuming it represents an intravascular region. The estimated AIF is then subsequently used in the region-by-region (each

region is 20x20 pixels) non-blind deconvolution of the whole image sequence to calculate the perfusion-parameter maps.

#### IV. EXPERIMENTAL DATA AND RESULTS

##### A. Experimental Data

a) *Animals*: The proposed AIF estimation method is evaluated on preclinical data. The test recordings (approved by the National Animal Research Authority) was done on a BALB/c mouse with murine colon tumor cells CT26.WT (ATCC, CRL-2638) subcutaneously implanted into the left flank ( $1 \times 10^6$  cells in HC Matrigel). Four mice were examined in the following way. Each mouse underwent three DCE-MRI examinations, two with a standard low-molecular-weight contrast agent (Magnevist, Bayer HealthCare Pharmaceuticals, Berlin, Germany) and one with a high-molecular-weight contrast agent (GadoSpin P, Miltenyi Biotec, Bergisch Gladbach, Germany). In addition, two of these mice underwent a DCE-US examination (contrast agent: Vevo MicroMarker, Visualsonics, Toronto, Canada).

b) *MRI acquisition*: One axial slice through the tumor middle was imaged. The mice were anesthetized with Isoflurane,  $O_2$  and monitored continuously for respiratory rate and body temperature. A 9.4T BioSpin (Bruker Biospin MRI, Ettlingen, Germany) scanner was used with the following acquisition parameters: 2D FLASH sequence with TR/TE 14/2.5 ms, flip angle 25 deg., image matrix 128x96 pixels, slice thickness 1 mm, sampling interval 1.05 s, acquisition time 13 min. Before the bolus administration, 15 images were recorded with TR = 14, 30, 50, 100, 250, 500 ms to convert the dynamic image sequence to the contrast-agent concentration. Anatomical images were recorded using the RARE sequence (T2-weighted and T1-weighted pre- and post-contrast).

c) *US acquisition*: A Vevo 2100 (Visualsonics, Toronto, Canada) scanner was used with the MS250 probe, nonlinear contrast imaging mode, acquisition time 2 min 40 s. To convert image intensity within the ROI to the concentration of the contrast agent, standard preprocessing is applied, including linearization of video data (conversion to envelope data) and square operation, see e.g. [15].

##### B. Results

The resulting DCE-MRI perfusion-parameter maps were spatially consistent and in the expected range. They showed the expected characteristics according to assumed histological composition. There was a clear distinction between the tumor rim and the fibro-necrotic centre. On the  $PS$  map the permeability decreased towards the centre. The  $F_b$  map was also with a good correlation with the expected malignant lesion features and other parametric images (not shown), the highest values on the outer lesion margin corresponded to the presence of the feeding and draining vessels.

The box plots in Figs. 3 and 4 show the perfusion-parameter estimates in manually drawn tumor ROIs. The central mark is the median, the edges of the box are the 25th and 75th percentiles, the whiskers extend to the most extreme data points not considered outliers. In line with theoretical

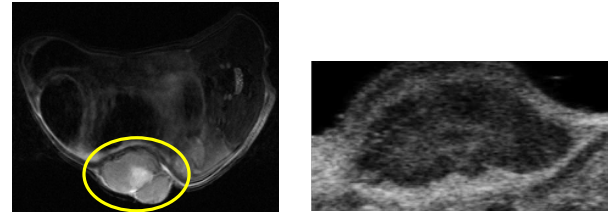


Fig. 1. Left: Example of T2-weighted anatomical image of the tumor, mouse 1, examination 2.. Ellipse denotes the tumor cross-section. Upper region is a cross-section of spine and spinal muscles. Right: Example of B-mode ultrasound image of tumor, mouse 1.

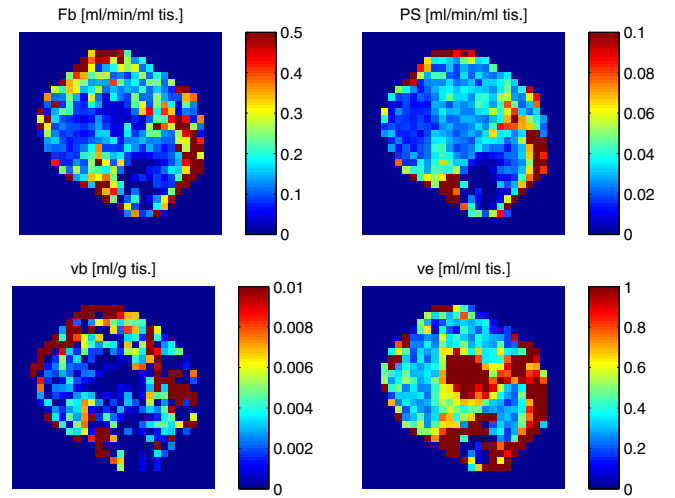


Fig. 2. Examples of estimated DCE-MRI perfusion-parameter maps within the tumor, mouse 1, examination 2.

expectations the estimates of  $F_b$  were independent of the contrast agent's molecular weight, while the estimates of  $PS$  showed lower values for the high-molecular-weight contrast agent. Reproducibility of the perfusion-parameter estimates (deduced from the comparison of the two Magnevist examinations) was fairly good (except for  $PS$ , mouse M04). Intersubject comparison indicates a fairly homogeneous animal group, except for mouse M04 with a clearly more perfused tumor giving consistently higher  $F_b$  and  $PS$  than for other animals.

The perfusion-parameter maps from DCE-US (Fig. 5) corresponded well with the DCE-MRI maps. Also the scale of blood flow was the same (box plots in Figs. 5 and Fig. 3).

#### V. CONCLUSIONS

Estimation of AIF using blind deconvolution is feasible, as was shown for DCE-MRI on clinical [8], [9] and preclinical data [2], [3]. The presented extension of blind-deconvolution DCE-MRI introduces the combination of an advanced pharmacokinetic model (ATH) and a new small-animal AIF model. This allows robust estimation of  $F_b$  and  $PS$  in addition to the Tofts-model's perfusion parameters. To evaluate the DCE-MRI method we have proposed a new way of indirect validation by using two contrast agents of different molecular weight. The presented extension of our DCE-US method towards pixel-wise perfusion analysis

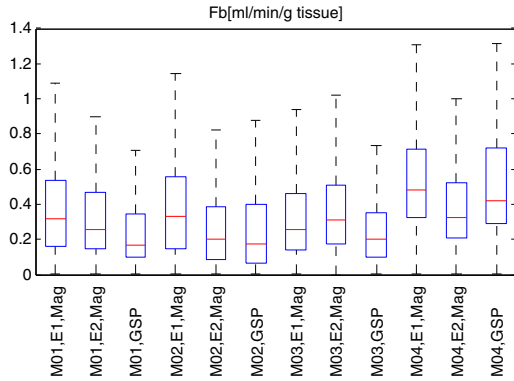


Fig. 3. Box plots of  $F_b$  within a the tumor region. M0X – animal number, EX – examination number, Mag – Magnevist, GSP - GadoSpin P

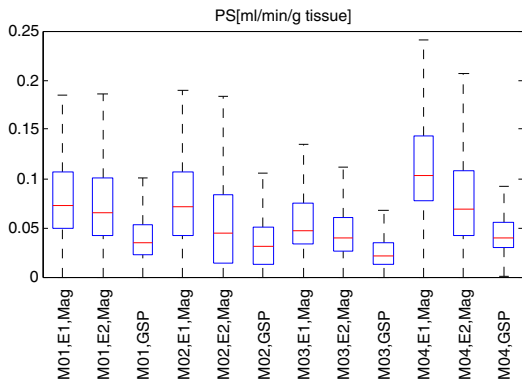


Fig. 4. Box plots of  $PS$  within a the tumor region. M0X – animal number, EX – examination number, Mag – Magnevist, GSP - GadoSpin P

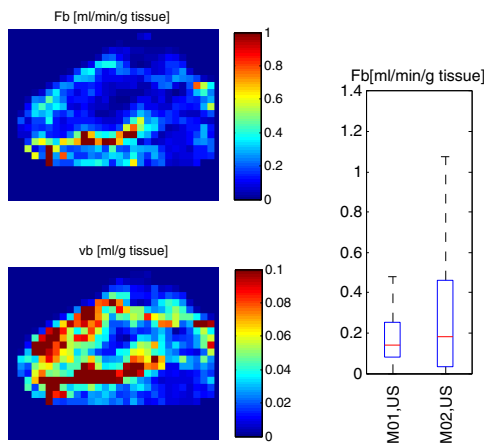


Fig. 5. Left: example of estimated DCE-US perfusion-parameter maps within the tumor, mouse 1. Right: box plots of  $F_b$  within the tumor region. M0X denotes animal number.

and combination with the new AIF model seems to give consistent results, when compared to DCE-MRI estimates of  $F_b$ . A thorough validation will be needed to assess the achievable accuracy and reproducibility of the methods.

## REFERENCES

- [1] S. P. Sourbron and D. L. Buckley, "Tracer kinetic modelling in MRI: estimating perfusion and capillary permeability," *Physics in medicine and biology*, vol. 57, no. 2, pp. R1–33, Jan. 2012.
- [2] O. Keunen, M. Johansson, A. Oudin *et al.*, "Anti-VEGF treatment reduces blood supply and increases tumor cell invasion in glioblastoma." *Proceedings of the National Academy of Sciences of the United States of America*, vol. 108, no. 9, pp. 3749–3754, Mar. 2011.
- [3] T. Taxt, R. Jirik, C. B. Rygh *et al.*, "Single-Channel Blind Estimation of Arterial Input Function and Tissue Impulse Response in DCE-MRI," *Biomedical Engineering, IEEE Transactions on*, vol. 59, no. 4, pp. 1012–1021, Apr. 2012.
- [4] M. M. Pike, C. N. Stoops, C. P. Langford *et al.*, "High-resolution longitudinal assessment of flow and permeability in mouse glioma vasculature: Sequential small molecule and SPIO dynamic contrast agent MRI." *Magnetic resonance in medicine*, vol. 61, no. 3, pp. 615–25, Mar. 2009.
- [5] M. E. Loveless, J. Halliday, C. Liess *et al.*, "A quantitative comparison of the influence of individual versus population-derived vascular input functions on dynamic contrast enhanced-MRI in small animals." *Magnetic resonance in medicine*, vol. 67, no. 1, pp. 226–236, Jan. 2012.
- [6] M. Verhoye, B. P. J. van der Sanden, P. F. J. W. Rijken *et al.*, "Assessment of the neovascular permeability in glioma xenografts by dynamic T1 MRI with Gadomer-17." *Magnetic resonance in medicine*, vol. 47, no. 2, pp. 305–13, 2002.
- [7] M. Heisen, X. Fan, J. Buurman, and B. t. H. Romeny, "Effects of reference tissue AIF derived from low temporal resolution DCE-MRI data on pharmacokinetic parameter estimation," in *ISMRM-ESMRMB Joint Annual Meeting 2010. - Sweden, Stockholm*, Stockholm, 2010, p. 4802.
- [8] D. Y. Riabkov and E. V. R. Di Bella, "Estimation of kinetic parameters without input functions: Analysis of three methods for multichannel blind identification," *IEEE Transactions on biomedical engineering*, vol. 49, no. 11, pp. 1318–1327, 2002.
- [9] J. U. Fluckiger, M. C. Schabel, and E. V. R. DiBella, "Model-Based Blind Estimation of Kinetic Parameters in Dynamic Contrast Enhanced (DCE)-MRI," *Magnetic resonance in medicine*, vol. 62, no. 6, 2009.
- [10] M. Mezl, R. Jirik, V. Harabis, and R. Kolar, "Quantitative ultrasound perfusion analysis in vitro," in *Proceedings of Biosignal 2010: Analysis of Biomedical Signals and Images*, vol. 20. Brno University of Technology, 2010, pp. 279–283.
- [11] M. Gauthier, F. Tabarout, I. Leguernes *et al.*, "Assessment of quantitative perfusion parameters by dynamic contrast-enhanced sonography using a deconvolution method: an in vitro and in vivo study." *Journal of ultrasound in medicine*, vol. 31, no. 4, pp. 595–608, 2012.
- [12] R. Jirik, K. Nylund, O. H. Gilja *et al.*, "Ultrasound perfusion analysis combining bolus-tracking and burst-replenishment." *IEEE transactions on ultrasonics, ferroelectrics, and frequency control*, vol. 60, no. 2, pp. 310–319, Feb. 2013.
- [13] R. Jirik, K. Nylund, T. Taxt *et al.*, "Parametric Ultrasound Perfusion Analysis Combining Bolus Tracking and Replenishment," in *Proceedings of the IEEE International Ultrasonics Symposium 2012*. IEEE, 2012, pp. 1323–1326.
- [14] M. Heilmann, C. Walczak, J. Vautier *et al.*, "Simultaneous dynamic T1 and T2\* measurement for AIF assessment combined with DCE MRI in a mouse tumor model." *Magma*, vol. 20, no. 4, pp. 193–203, 2007.
- [15] N. G. Rognin, P. Frinking, M. Costa, and M. Arditi, "In-vivo perfusion quantification by contrast ultrasound: Validation of the use of linearized video data vs. raw RF data," in *IEEE Proceedings of Ultrasonics Symposium*. IEEE, 2008.